Ab initio cross sections for low-energy inelastic H+Na collisions

A. K. Belyaev
Departement of Theoretical Physics, Pedagogical University of Russia, St. Petersburg 191186, Russia

J. Grosser, J. Hahne, and T. Menzel
Institut für Atom- und Molekülphysik, Universität Hannover, 30167 Hannover, Germany

(Received 23 March 1999)

We report *ab initio* results for the integral cross section of the process $H+Na(3s)\rightarrow H+Na(3p)$ for collision energies from the threshold (2.1 eV) to 600 eV. We achieve a reasonable agreement with the experimental data, which are available for energies above 10 eV. The main contributions to the cross section come from a rotational coupling mechanism in the NaH triplet molecular system and from a curve-crossing mechanism in the singlet system. At very low energy (2.1–2.4 eV), the process is governed by a centrifugal barrier in the exit channel leading to orbital resonances. The Landau-Zener model provides a reasonable qualitative description of the radial coupling mechanism at high energies, but fails below 10 eV. [S1050-2947(99)05509-2]

PACS number(s): 34.50.Fa, 34.20.Mq

I. INTRODUCTION

Inelastic collisions between thermal atoms, molecules, or ions are decisive for the properties of nonequilibrium gaseous media such as planetary or stellar atmospheres, gaseous laser media, and laboratory plasmas. There is consequently a constant demand for cross-section data for low-energy inelastic collisions. In the great majority of cases, the required data are not available. Cross sections can be obtained both from experiments and from numerical calculations. Experiments in this field are often very difficult. For instance, low-energy (few eV) neutral atom beams are difficult to produce and control, leading to the fact that atom-atom collisions have been investigated in this energy range only for a small number of experimentally favorable cases. Numerical calculations, on the other hand, seem to offer no principal difficulties, nevertheless the number of theoretical papers dealing with low-energy atomic or ionic collisions is very small, probably because there are usually no corresponding experiments.

The process investigated in the present paper is of interest in particular for applications in astrophysics. Stellar photospheres are often satisfactorily described by local thermal equilibrium (LTE) models; data on inelastic collisions are not required under these conditions. Considerable deviations from LTE have been observed in a variety of cases, for instance in red giant stars such as Pollux (βGem); collisional excitation of atoms by hydrogen-atom impact is believed to be of considerable importance for the photospheres of these stars. The construction of photospheric models is, however, highly tentative, because even the order of magnitude of the relevant cross sections is unknown [1,2]. The main interest is in the collisions of hydrogen atoms, which form the main constituent of stellar photospheres, with other photospheric atoms such as Fe, Ca, Ca^+, Ba^+, and Na at energies slightly above the excitation threshold, which is a few eV. We decided to study the process

$$H+Na(3s)\rightarrow H+Na(3p) \qquad (1)$$

first, because this is one of the few cases for which low-energy experimental data [3] are available.

Except for extremely small energies, the de Broglie wavelength of an atom is small compared to the typical atomic distances. Therefore, the motion of the atoms is close to classical under many aspects. This has led to theoretical formulations in which the atomic nuclei are supposed to move on a classical trajectory (CT), and only the electrons are treated quantum mechanically. CT methods have been applied in a great number of cases to high-energy atomic or ionic collisions. CT methods fail at lower energies, however. They are usually not applied at collision energies much below 1 keV, and they are certainly not applicable for the present energy range of interest. We use in the present work a quantum-mechanical approach for both the electronic and the heavy particle motion.

II. GENERAL FORMULATION

A. Coupled-channel equations

The present approach is essentially that of the eigenfunction [perturbed stationary states (PSS)] expansion described by Mott and Massey [4]. For details of the following discussion, see [5]. We neglect the spin-orbit interaction throughout the paper. The spin does not appear, therefore, except in the multiplicity quantum number; see below. Let **R** be the vector connecting the atoms, with R, θ, Φ the corresponding polar coordinates, and let $|j,\Lambda,s\rangle$, $j=1,\ldots,$ be electronic eigenfunctions of the collisional system, where $\Lambda\geqslant 0$ is the absolute value of the projection quantum number for the electronic orbital angular momentum upon the molecular axis, and $s=\pm 1$ stands for the reflection symmetry at a plane through the internuclear axis. The eigenfunctions depend on the internuclear distance R as a parameter. In numerical applications one has to rely on a truncated basis. The lowest molecular states of the NaH system are Σ^+ ($\Lambda=0$, $s=+1$) and Π ($\Lambda=1$, $s=\pm 1$) states. We do not consider other states at present. The total (electronic plus nuclear) wave function can be expressed under these conditions as a sum,

$$\Psi=\sum_{j,\Lambda}\frac{F^L_{j,\Lambda}(R)}{R}\Theta^L_{0\Lambda}(\theta)\,|j,\Lambda,+1\rangle\quad, \tag{2}$$

with $\Lambda=0,1$. L is the quantum number for the total (electronic plus nuclear) angular momentum. The corresponding projection quantum number is chosen to be zero in order to meet the usual scattering boundary conditions. The $\Theta^L_{0\Lambda}$ are generalized spherical harmonics, which describe the angular motion of the atoms, and the $F^L_{j,\Lambda}$ describe the radial motion. The fact that no states $|\Pi,-1\rangle$ appear here reflects the conservation of reflection symmetry: a collision starting in a Σ^+ state cannot result in Π states which have negative reflection symmetry at the scattering plane. In what follows, the indices L,Λ,s are not indicated any more, unless necessary. The radial functions obey a system of coupled-channel equations,

$$\left[-\frac{\hbar^2}{2M}\frac{d^2}{dR^2}+V^{\rm eff}_j(R)-E\right]F_j$$
$$=\frac{\hbar^2}{M}\sum_{k\neq j}\langle j|\frac{\partial}{\partial R}|k\rangle\frac{dF_k}{dR}+\frac{\hbar^2}{2M}\sum_k\langle j|\frac{\partial^2}{\partial R^2}|k\rangle F_k$$
$$+\frac{\hbar}{MR^2}\sum_k\sqrt{L(L+1)}\,(\Lambda_k-\Lambda_j)\,\langle j|i\,L_y|k\rangle F_k\,. \tag{3}$$

M is the reduced mass of the colliding atoms, E is the total energy, and $V^{\rm eff}_j(R)$ is the effective potential,

$$V^{\rm eff}_j(R)=V_j(R)+\frac{\hbar^2[L(L+1)-\Lambda^2]}{2MR^2}, \tag{4}$$

that is, the sum of the adiabatic potential $V_j(R)$ and the centrifugal energy. L_y and $L_\pm$ are the components of the electronic angular momentum operator with respect to body-fixed coordinates [5]. In Eq. (3), terms with the matrix elements $\langle j|L_+L_-+L_-L_+|k\rangle$ have been omitted as being negligible; see below. The coupling matrix elements, which appear on the right-hand side of Eq. (3), are responsible for the transitions between different electronic states j and k. It is worth pointing out that the first two sums on the right-hand side of Eq. (3) couple molecular states of the same symmetry, while the last sum couples Σ and Π states. The NaH collisional molecule possesses singlet and triplet electronic states which, due to the neglect of the spin-orbit interaction, do not couple at all. We deal therefore with two distinct systems of coupled equations.

We take the potentials and the coupling matrix elements, which are required to set up Eq. (3), from *ab initio* quantum chemical calculations. Standard quantum chemical programs usually provide, in addition to the potentials, reliable values for the rotational ($i\,L_y$) and the single derivative ($\partial/\partial R$) matrix elements in Eq. (3), but not for the double derivative matrix elements $\langle j|\partial^2/\partial R^2|k\rangle$. In the present case, only the single derivative matrix element and the rotational couplings are of major importance. This is not generally true, but it holds in many similar cases. The important point is that in the present case, the $\langle j|\partial/\partial R|k\rangle$ matrix elements do not exceed the order of a_0^{-1}, with a_0 the Bohr radius (see below). We conclude that $\partial/\partial R|k\rangle$ has the order of $a_0^{-1}|k\rangle$ for all states in question, and hence $\langle j|\partial^2/\partial R^2|k\rangle$ is of the order of a_0^{-2}. The operation dF_k/dR multiplies the nuclear wave function typically by the local wave number

$$\kappa_k(R)=\sqrt{\frac{2M}{\hbar^2}[E-V^{\rm eff}_k(R)]}\,. \tag{5}$$

The typical values of κ_k are much larger than a_o^{-1}, which means that the first coupling term in Eq. (3) is much larger than the second one. This suggests the neglect of the second coupling term. It turns out, however, that Eq. (3) without the second coupling term violates particle conservation. A complete neglect of this term is therefore not advisable, but a rough approximation should be sufficient. The coupling matrix elements are easily shown to obey the following relations:

$$\langle j|\frac{\partial^2}{\partial R^2}|k\rangle-\langle k|\frac{\partial^2}{\partial R^2}|j\rangle=2\frac{d}{dR}\langle j|\frac{\partial}{\partial R}|k\rangle, \tag{6}$$

$$\langle j|\frac{\partial^2}{\partial R^2}|k\rangle=\frac{d}{dR}\langle j|\frac{\partial}{\partial R}|k\rangle+\sum_m\langle j|\frac{\partial}{\partial R}|m\rangle\langle m|\frac{\partial}{\partial R}|k\rangle. \tag{7}$$

In order to obtain double derivative matrix elements from the calculated single derivative matrix elements, we use the following approximation:

$$\langle j|\frac{\partial^2}{\partial R^2}|k\rangle=\frac{d}{dR}\langle j|\frac{\partial}{\partial R}|k\rangle. \tag{8}$$

The approximate matrix elements obey Eq. (6) and therefore guarantee particle conservation. What is actually neglected is the sum in Eq. (7). Coupling terms, which are proportional to the matrix elements of $(L_+L_-+L_-L_+)$, appear in Eq. (3) as well; they are of the same order as the double derivative matrix elements and their neglect causes no comparable problems.

The coupling matrix elements seem to be unambiguously defined, at first sight. However, it is well known that their values depend on the choice of the electron coordinate origin [6,7]. We use here matrix elements, which are calculated with the origin of the electron coordinates at the Na atom; actually, this lets the $\langle j|\partial/\partial R|k\rangle$ disappear as $R\to\infty$ for all channels considered at present. Formally, the problem occurs because the operation $\partial/\partial R$ is a partial differentiation, which is unambiguously defined only when it is specified which other quantities (here electron coordinates) are held constant. Physically, the problem is related to what is known as ''electron translation'' and is solved by the introduction of ''electron translation factors'' in CT approaches. Methods for the solution of the electron translation problem in the framework of the full quantum approach have been discussed [6]; the practical experience with these methods is very limited [8,9]. We have recently proposed another approach [10] to this problem. A preliminary application to the H+Na case shows that, compared to the present results, the corrections do not exceed the order of a few percent.

B. Numerical procedures

For the numerical solution of Eq. (3), the number of basis states $|j\rangle$ is truncated to a finite number N (three or four at present). This reduces Eq. (3) to N coupled equations. The solutions have to obey the following boundary conditions:

$$F_j(R)\rightarrow 0 \text{ as } R\rightarrow 0 \text{ for } j=1,\ldots,N \tag{9}$$

and

$$F_j(R)\rightarrow \frac{\delta_{j1}}{\sqrt{k_j}}e^{-ik_jR}+\frac{a_j}{\sqrt{k_j}}e^{+ik_jR} \text{ as } R\rightarrow\infty \text{ for } j=1,\ldots,N \tag{10}$$

with

$$k_j=\sqrt{\frac{2M}{\hbar^2}[E-V_j(\infty)]}\,. \tag{11}$$

The quantities a_j represent the outgoing amplitudes in the different atomic states. Practically, the first condition means that the wave functions have to go rapidly to zero in the classically forbidden region where $E-V_j^{\text{eff}}$ is negative. For the numerical treatment, we define a value R_{start} of the internuclear distance, which is classically forbidden for all channels, that is, $E-V_j^{\text{eff}}(R_{\text{start}})<0$ for all j. For $R<R_{\text{start}}$, the radial functions F_j are approximated as WKB functions [11]. For $R_{\text{start}}<R<R_{\text{stop}}$, with R_{stop} typically between 25 and 40 a.u., we compute N linearly independent real solutions of Eq. (3), using Numerical Algorithms Group (NAG) routines for the numerical integration. Beyond R_{stop}, the solutions are continued to infinity using again WKB functions. The values R_{start} and R_{stop} are chosen in such a way that they are without influence on the final results. The numerical solutions have a tendency to diverge, especially in the region where only a part of the channels is classically allowed. This can lead to numerical difficulties; they are prevented by forming better suited linear combinations at intermediate values of R. The N solutions are finally linearly combined to find the solution obeying Eq. (10) and, hence, giving the outgoing amplitudes a_j. The transition probabilities are obtained from the outgoing amplitudes as

$$P_j=|a_j|^2\,. \tag{12}$$

They represent the ratio between the outgoing radial current in the excited-state number j and the incoming current in the ground state $j=1$ at $R\rightarrow\infty$. The integral cross sections are calculated as partial wave sums with the statistical weights of $\frac{1}{4}$ and $\frac{3}{4}$ for the singlet and triplet states, respectively. Except for very low energies, a large number of L values contribute to the cross section, giving L the character of a quasicontinuous variable. At higher energy, L is replaced by the impact parameter b, defined as

$$b=\sqrt{L(L+1)}/k_1\,, \tag{13}$$

and the cross sections were computed as integrals over the impact parameter.

The present work forms the continuation of similar earlier work [12–14]. The main difference from our earlier work is that the coupled equations are now solved numerically as they stand; the WKB approximation does not enter. We use WKB expressions only to extrapolate our numerical solutions to $R\rightarrow 0$ and to $R\rightarrow\infty$, respectively. This is without influence on the results. The results for the wave functions, for the transition probabilities, and for the cross sections obtained in this way represent exact solutions of the truncated coupled equations.

We use several concepts for the interpretation of the numerical data. Besides the channel wave functions $F_j(R)$ and the transition probabilities P_j, these are the incoming, $J_j^-(R)$, and outgoing, $J_j^+(R)$, currents. For the currents we use the definitions [13]

$$J_j^{\pm}=|F_j^{\pm}|^2,\qquad F_j^{\pm}=\kappa_j^{+1/2}F_j\pm i\kappa_j^{-1/2}\frac{dF_j}{dR}, \tag{14}$$

where $\kappa_j(R)$ is determined by Eq. (5). They are meaningful as long as the channel wave functions F_j can be discussed, at least qualitatively, as WKB functions; when the WKB approximation is valid, one has

$$F_j(R)=\kappa_j^{-1/2}[F_j^+e^{+i\Phi_j(R)}+F_j^-e^{-i\Phi_j(R)}] \tag{15}$$

with $\Phi_j=\int^R\kappa_j dR$. This clearly gives J_j^+ and J_j^- the meaning of incoming and outgoing currents with the obvious relation $P_j=J_j^+(\infty)$.

III. RESULTS

A. Quantum chemical data

The adiabatic potentials and the coupling matrix elements are calculated by the multireference single- and double-excitation configuration-interaction (MRD-CI) method [15,16]. We use an H(12*s*,8*p*,2*d*)Na(13*s*,9*p*,2*d*) Gaussian basis contracted to H(9*s*,6*p*,1*d*)Na(7*s*,5*p*,2*d*), which is similar to the one used in Ref. [16]. The lowest NaH adiabatic potentials are shown in Figs. 1(a) and 1(b), the radial couplings in Figs. 1(c) and 1(d), and the rotational coupling matrix elements in Figs. 1(e) and 1(f). The panels at the left- and right-hand sides represent the NaH singlet and triplet states, respectively. In Figs. 1(a) and 1(b), the solid lines are Σ states, the dashed lines represent the lowest Π states, the thick lines are the potentials calculated in the present work and indicate the states taken into the present dynamical calculation, and the thin lines are the potentials from Ref. [16]. The calculated asymptotic values ($R\rightarrow\infty$) of the potentials deviated from the true atomic values, originally. We constructed smooth corrections in the region $R>20$ a.u.; the corrections amounted to 0.08 eV for the H+Na(3*p*) asymptote and 0.25 eV for H+Na(4*s*).

Inelastic transitions can occur in a region where a close approach of potential curves takes place together with a large value of the corresponding coupling matrix element. The NaH quasimolecule has a number of such regions. Figure 1(a) shows that the NaH singlet system is governed by a series of avoided crossings, as the strongly attractive ion pair (Na^+H^-) potential curve crosses a number of curves representing Na(nl)+H(1*s*) states (see also Ref. [16]). These crossings represent indeed a major mechanism for the inelas-

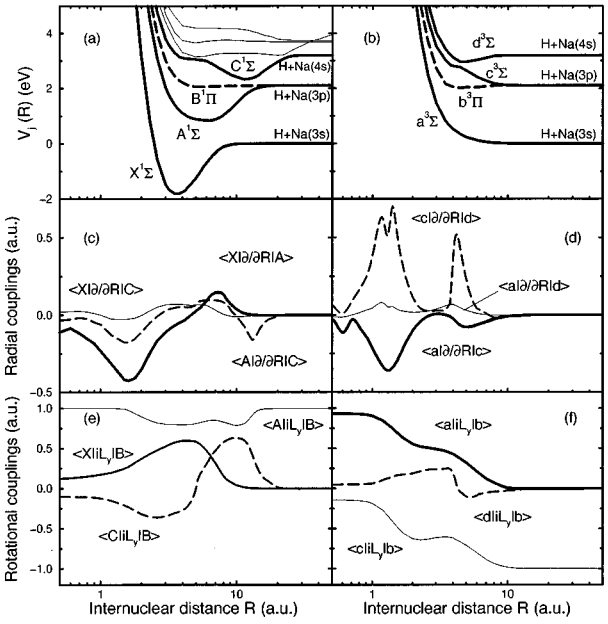

FIG. 1. NaH quantum chemical data. The figures on the left- and on the right-hand sides correspond to singlet and triplet states, respectively. (a) and (b) The adiabatic potentials. The solid lines show the Σ states, the dashed lines depict the Π states. The thick lines represent the states used in the present calculations. (c) and (d) Radial coupling matrix elements, (e) and (f) rotational coupling matrix elements.

tic process in question. When one passes through an avoided crossing region, the electronic wave functions exchange their character. The lowest potential curve in Fig. 1(a), $X\,^1\Sigma$, should therefore represent the configurations Na^+H^- and $Na(3s)H(1s)$ to the left- and right-hand sides of the crossing region, respectively. The corresponding variation of the electronic wave function with the internuclear distance should give rise to a peak in the matrix element $\langle X\,^1\Sigma|\partial/\partial R|A\,^1\Sigma\rangle$, which is indeed clearly visible in Fig. 1(c) near the corresponding internuclear distance $R\approx 7.4$ a.u. However, in the usual (Landau-Zener) model descriptions of an avoided crossing, one has [7]

$$\left|\int \langle 1|\frac{\partial}{\partial R}|2\rangle\, dR\right| = \frac{\pi}{2}. \tag{16}$$

The corresponding integral over the nonadiabatic region around $R\approx 7.4$ a.u. is found to be considerably smaller, about half as large, indicating that the avoided crossing interpretation cannot be expected to provide more than a qualitative description. The avoided crossing between the $A\,^1\Sigma$ and $C\,^1\Sigma$ molecular states appears in a similar way, providing another nonadiabatic region near $R\approx 13.2$ a.u. The absolute value of the corresponding integral is too small again. These conclusions are in agreement with Ref. [7]. At small distances, large values of the matrix element $\langle X\,^1\Sigma|\partial/\partial R|A\,^1\Sigma\rangle$ occur; see Fig. 1(c). They are not expected to provide an efficient mechanism for the inelastic process (1), because the energy gap between the $X\,^1\Sigma$ potential and the other potential curves remains large even at the smallest distances, as demonstrated by Fig. 2, where the potential differences are shown. Similarly, the $B\,^1\Pi - X\,^1\Sigma$ energy gap remains large,

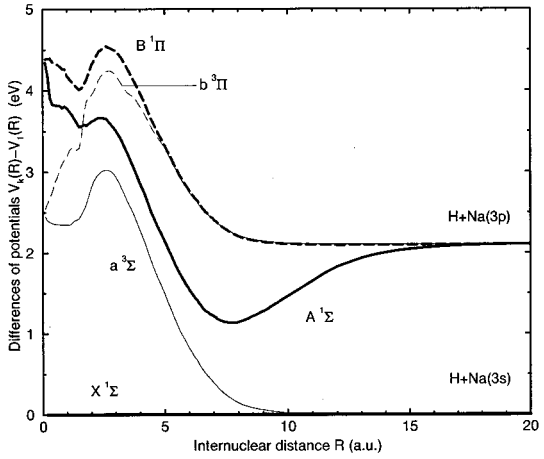

FIG. 2. Differences between the adiabatic potentials $V_k(R)$ of low-lying excited states and the ground-state potential $V_1(R)$ for the singlet (the thick lines) and triplet (the thin curves) NaH systems. The solid lines correspond to the Σ states, while the dashed ones correspond to the Π states.

such that for the singlet system, rotational coupling is not expected to provide an efficient coupling between the ground state and excited states.

The adiabatic potentials for the triplet system show an entirely different behavior; see Figs. 1(b) and 2. Due to the absence of a triplet ion pair state, there is no series of avoided crossings at large internuclear separations. The $a\,^3\Sigma$ potential curve does not approach the nearest excited $c\,^3\Sigma$ curve (Fig. 2), such that radial coupling is expected to be ineffective for the process (1). However, at small internuclear distance the $a\,^3\Sigma$ and $b\,^3\Pi$ potential curves come very close to each other. The system appears to converge to the united atom limit, $Mg(3s3p\,^3P)$, where one expects indeed a Σ-Π degeneracy. Together with the large rotational coupling, the approximate degeneracy is expected to provide a very effective rotational mechanism for nonadiabatic transitions [17–19]. The same kind of degeneracy exists for the singlet $A\,^1\Sigma$ and $B\,^1\Pi$ states (Fig. 2), which, combined with the large value of the corresponding rotational coupling, is expected to give transitions between these states at small internuclear distances.

B. Cross sections and basic mechanisms

Figure 3 shows our results for the integral cross sections. The numerical calculations were carried out with a four-state basis for the singlet as well as for the triplet system for energies above 3.2 eV. The results demonstrate that at low energy, essentially only one process is of importance, $Na(3p)$ production in the singlet system. We disregard the triplet system below 3.2 eV, therefore, and we use only a three-state basis ($X\,^1\Sigma$, $A\,^1\Sigma$, and $B\,^1\Pi$) for the singlet system at these energies.

The incoming and outgoing currents turn out to be an efficient tool for understanding the mechanisms of the process. Typical numerical results for these quantities are shown in Fig. 4, which gives a good idea of the basic mechanisms. In order to make the data more illustrative, the currents are represented by the thickness of the lines in the effective po-

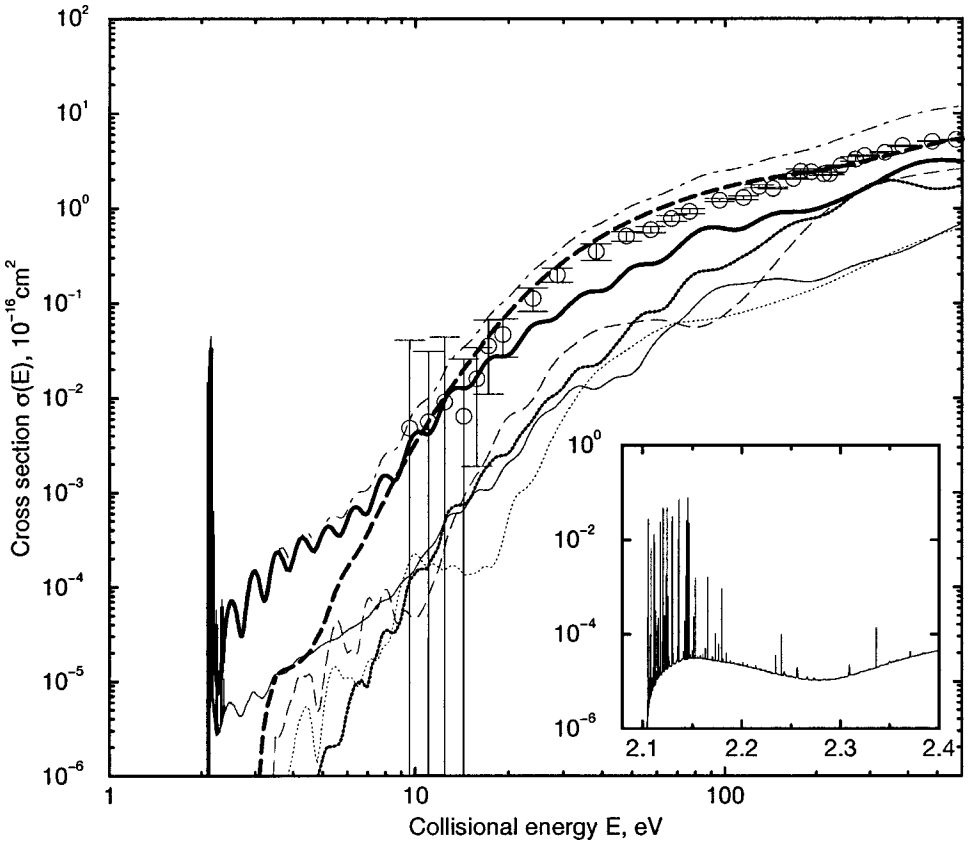

FIG. 3. NaH integral inelastic collision cross sections as a function of the collisional energy. The symbols are the experimentally measured $3p \rightarrow 3s$ emission cross section, the lines are the calculated excitation cross sections. The thick and the thin solid lines are the partial Na($3p\sigma$) and Na($3p\pi$) excitation cross sections in the singlet system, the thick dotted line is the Na($4s\sigma$) excitation cross section in the singlet system, the thick and the thin dashed lines are Na($3p\pi$) and Na($3p\sigma$) cross sections in the triplet system, and the thin dotted line is the Na($4s\sigma$) cross section in the triplet system. The dot-dashed curve is the total Na($3p$) excitation cross section. The inset shows the total Na($3p$) cross section near the threshold on an enlarged scale.

tential curve diagrams. In the singlet system, the incoming [Fig. 4(a)] and outgoing [Fig. 4(c)] currents are exchanged between the ground state and the first excited state primarily in the avoided crossing region at 7.4 a.u., populating mainly the $A\,^1\Sigma$ state. It is remarkable that apparently no radial coupling transitions occur at small distance, though the radial coupling matrix elements are very large in this region; see Fig. 1(c). Obviously, for an effective coupling mechanism, a close approach of the potentials is required in addition to a large coupling. In the triplet system, in contrast, the exchange occurs at a much smaller distance, and essentially only the $b\,^3\Pi$ state is populated; see Figs. 4(b) and 4(d). This is indeed what one expects for the rotational coupling mechanism near the united atom limit described above. Secondary transitions are responsible for the population of higher excited states. For instance, in the singlet system the outgoing current flows from the $A\,^1\Sigma$ state to the $C\,^1\Sigma$ state at the avoided crossing near 13.2 a.u. A small outgoing current in the $B\,^1\Pi$ state, which is produced by small distance rotational coupling, is also remarkable.

Figure 5 shows the transition probabilities as a function of the impact parameter for both the singlet and the triplet systems. It is seen that the transitions in the singlet system occur for an impact parameter range between 0 and 8 a.u. [Fig. 5(a)]. For the triplet system, the range is much smaller [Fig. 5(b)]. This is natural, because a much closer approach of the atoms is required. The oscillations in the singlet transition probability are the well-known Stückelberg oscillations, which occur by interference between the two possibilities for the process, with a transition at the first or the second passage through the radial coupling region. The triplet system shows no such structures, because the transition region is close to the classical turning point. The higher excited states in the singlet system show similar Stückelberg oscillations, because they are populated indirectly from the outgoing current in the lowest excited state.

In the integral cross section, one observes dominant population of two channels, $b\,^3\Pi$ and $A\,^1\Sigma$. The first one dominates at high collision energy, the second one at low energy. The oscillations of the cross sections reflect the Stückelberg oscillations of the transition probabilities [Fig. 5(a)] once more. They are damped due to the integration over the impact parameter, but they do not disappear completely, in particular at low energy. In a small region near the threshold, resonance peaks are superimposed on the continuous cross-section curve (see the inset in Fig. 3). Depending on the impact parameter, the effective potential of the $A\,^1\Sigma$ state possesses a centrifugal barrier. When a transition to the excited state occurs at a kinetic energy below the barrier, the collisional system is caught inside the barrier. Except for tunneling, the barrier cannot be passed, so that the system eventually decays back to the ground state. Tunneling is

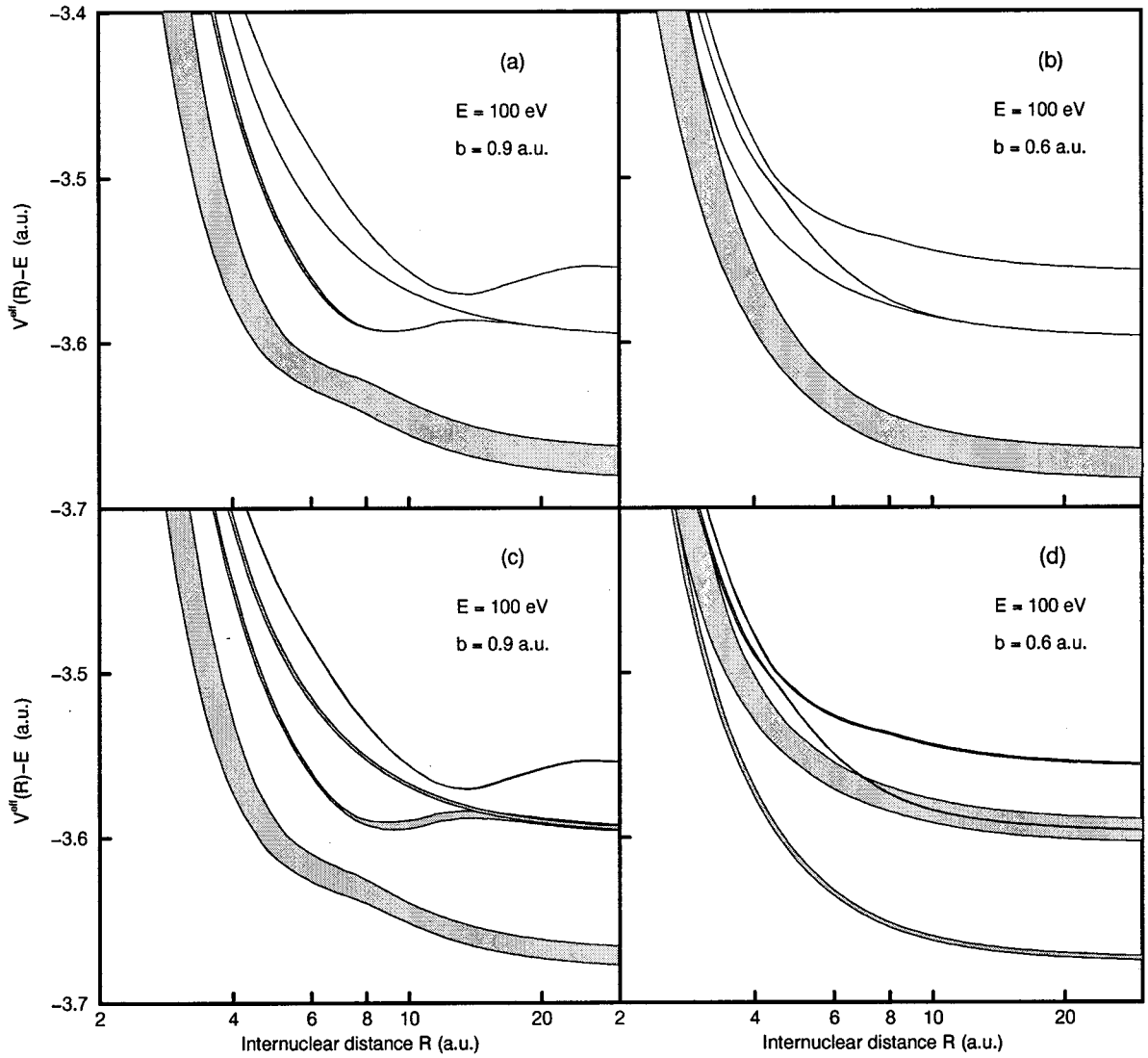

FIG. 4. Incoming (a,b) and outgoing (c,d) currents in the different electronic singlet (a,c) and triplet (b,d) states for the collisional energy $E=100$ eV. The magnitudes of the currents are represented by the thickness of the curves corresponding to $V_j^{\mathrm{eff}}(R)-E$.

quite ineffective in this situation, such that one expects a small inelastic cross section, generally. However, when the energy coincides with that of a quasibound state, the amplitude behind the barrier can become very large, resulting in a correspondingly large outgoing current and hence a large cross section. This gives rise to the resonance structures. The cross section on a resonance peak can be several orders of magnitude larger than the cross section for the nonresonant process. However, the resonances are extremely narrow, in general narrower than the line thickness in Fig. 3. We estimate that there are about 100 clear resonance peaks. For some cases, as in investigations of a thermal ensemble such as a stellar atmosphere, only the average cross sections are of interest. For the process (1), the cross section averaged over the resonances is about 15% above the nonresonant part of the low-energy cross-section curve.

It is tempting to describe the transitions at the avoided crossings using nonadiabatic models, in particular using the Landau-Zener model. We calculated an integral cross section on this basis. We used the Landau-Zener formula for the transition probability; the parameters were estimated from the form of the potential curves. No other approximations were used in this computation. The cross section obtained in this way turns out to be in qualitative agreement with the numerical result for the singlet system at collisional energies above 10 eV. However, the Landau-Zener model overestimates the integral cross section by a factor of 2 to 4 in this region. We ascribe this to the fact that the actual radial coupling is smaller than it should be according to the Landau-Zener model; see Eq. (16). Below 10 eV, the discrepancy between numerical and Landau-Zener results becomes larger and larger; the Landau-Zener model predicts a cross section near the threshold, which is smaller by several orders of magnitude than the numerical result. In the energy range between 3 and 5 eV, the transitions occur mainly for large impact parameter, or, classically speaking, at grazing incidence, quite in contrast to the predictions of the Landau-Zener model. Nonadiabatic transitions by radial coupling at grazing incidence were discussed previously [20]; the present case might form an interesting model system.

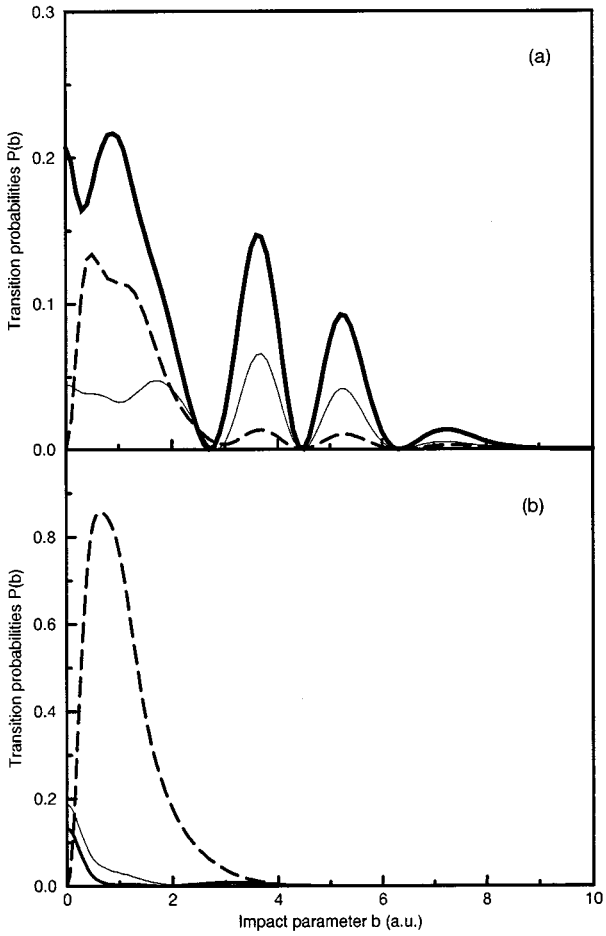

FIG. 5. The transition probabilities as a function of the impact parameter for the singlet (a) and triplet (b) systems at $E=100$ eV. The thick solid lines depict transition probabilities for excitation of the Na($3p\sigma$) state, the thin solid lines represent probabilities for excitation of the Na($4s\sigma$) state, and the dashed lines correspond to excitation of the Na($3p\pi$) state.

IV. GENERAL DISCUSSION: COMPARISONS AND ACCURACY

Experimental data for the Na($3p\rightarrow 3s$) and Na($4p\rightarrow 3s$) emission cross sections in H+Na($3s$) collisions at collisional energies above 10 eV are available [3]. The emission cross sections include cascade contributions, e.g., the collisional production of Na($4s$) with subsequent optical transitions $4s\rightarrow 3p$ and $3p\rightarrow 3s$. The emission cross sections are not calculated directly in the present work. Based on preliminary evaluations of the higher crossings [Fig. 1(a)], we estimate that a computed $3p\rightarrow 3s$ emission cross section would be typically 10% above the computed $3p$ production cross section (the uppermost curve in Fig. 3). In particular, a considerable fraction of what appears as $4s$ production in the singlet system in Fig. 3 is expected to result in ion pairs H^-+Na^+, when the higher crossings are taken into account. Comparing the calculated $3p$ cross section with the experimental data, we find that the general shape of the $3p\rightarrow 3s$ emission cross-section curve is very well reproduced. However, the computed value is above the experimental one by a factor of 2, except for the 10 eV region. In view of the variation of the cross section by three orders of magnitude over this range, we consider this as a good agreement.

The potentials calculated in the present work are in good agreement with other quantum chemical results [7,16,21] and with spectroscopic data [22]. For instance, our $A\,^1\Sigma-X\,^1\Sigma$ splitting at the avoided crossing is 1.14 eV compared to 1.21 eV from Ref. [21]. The calculated couplings are in good or reasonable agreement with those obtained by other authors; for instance, the peak of the radial coupling matrix element $\langle X\,^1\Sigma|\partial/\partial R|A\,^1\Sigma\rangle$ reported in Ref. [7] agrees within 10% with our value; the value of Ref. [23] is 25% larger. Some discrepancy exists with the triplet data reported in Ref. [24]. The relative signs of the radial coupling matrix elements are not consistent with ours. We checked our data carefully to make sure that they are correct.

Numerical calculations of cross sections were reported previously in Ref. [24], however only for the energy region above 200 eV. The authors used a CT approach and they did not consider rotational couplings. In view of the second point, their results must be too small; the calculated cross sections are indeed typically a factor of 2 below the experimental ones. Other work on the NaH system concentrated on the H^-+Na^+ channel [23] and is therefore not suited for direct comparison.

There are two principal possible origins for errors in the numerical results, the limited precision of the quantum chemical data and errors related to our treatment of the dynamics. We consider in particular the following possible causes for errors.

(i) Limited precision of the potentials. Generally, the calculated potentials are believed to be correct within about ± 0.1 eV, and errors are expected to be more significant in the asymptotic region ($R\rightarrow\infty$) than at small distances [16]. This is confirmed by the agreement achieved with the asymptotic atomic energy levels, as well as by the comparison with other calculations [7,16,21] and with spectroscopic data [22]. Numerical tests with modified potentials indicate that the integral cross-section data are sensitive especially to the energy differences. When, for instance, the potential difference in the crossing region of the singlet system is modified by 0.1 eV, the corresponding cross section can change by as much as 50%. This is similar for the rotational coupling mechanism in the triplet system. The height of the potential barrier in the exit channel, which is decisive for the cross section in the threshold region, depends critically on the detailed form of the $A\,^1\Sigma$ potential curve in this region. The cross-section curve between the threshold and 2.4 eV is certainly qualitatively correct, but the detailed behavior, e.g., the location of the resonances, might be subject to substantial errors.

(ii) The single derivative coupling matrix elements are believed to be correct within ± 0.015 a.u. [16]. Compared to the typical value of 0.2 a.u. of the matrix elements, this seems to imply errors not exceeding the order of 10% of the calculated cross section. Test calculations show that this is indeed true for not too low energies, $E>5$ eV. For the lowest energies, where the transition probabilities are extremely small, the numerical results depend very critically on details of the form of the radial coupling matrix elements. Corrections, which are significantly smaller than the expected pre-

cision of the quantum chemical data, can lead to large corrections in the calculated cross section. The reliability of our results in this energy range is difficult to judge, therefore, but we feel that possible errors should not exceed a factor of 2.

(iii) The use of Eq. (8) for the double derivative matrix element. Numerical tests using $\langle j|\partial^2/\partial R^2|k\rangle = 2\, d/dR\langle j|\partial/\partial R|k\rangle$ and $\langle k|\partial^2/\partial R^2|j\rangle = 0$ resulted in modifications of the cross section, which are of the order of a few percent at high energy ($E > 10$ eV), but can reach 25% in the low-energy region.

(iv) Truncation of the electronic basis. It appears unlikely that a treatment with four electronic basis states should be sufficient at high collision energy. The good qualitative agreement between experiment and theory seems to indicate, however, that at least the basic mechanisms of the process are correctly described. The remaining task is to increase the number of basis states and, in particular, to include continuum states into the coupled-channels approach. Experimental data for the ionization process ($H+Na \rightarrow H+Na^+ + e$) would be helpful to discuss this question further. At low energy, on the other hand, the limitation to a small basis should be adequate. This is supported by numerical evidence: calculations with an even smaller basis at low energy do not give significantly different results.

(v) Neglect of electron translation effects. Electron translation can be treated by using a large enough basis, as shown recently [10]. For the present system, the corrections are expected to be in the percent region only. It should be noted, however, that this approach faces difficulties again when electronic continuum states are to be included. In particular, in order to describe the translation of the active electron with the H atom (which takes part during a part of the processes under consideration), it might be necessary to include H^- continuum states.

V. CONCLUSION

Integral cross sections for the electronic excitation of Na atoms under H atom impact have been calculated for energies between the threshold and 600 eV. The potentials and the radial and rotational nonadiabatic coupling matrix elements were taken from quantum chemical calculations. The programs used for this purpose are working on the configuration interaction level. They were developed originally for the typical applications of quantum chemistry but turn out to be applicable for the present purposes, as well. The numerical treatment of the dynamics (i.e., the heavy particle motion) follows a full quantum approach based on the expansion of the wave function in terms of a finite number of molecular adiabatic states. We achieve a reasonable agreement between experiment and theory. The variation of the experimental cross section over three orders of magnitude is very well reproduced by the numerical results. The deviation of up to a factor of 2, which occurs at high energies, is probably due to the limitation to a too small electronic basis. The low-energy results, which are the main goal of the present activities, are expected to be less affected by truncation. For the lowest energies, the numerical calculations encounter another difficulty, the insufficient precision of the quantum chemical data. For a reliable computation of the very small cross sections of the present process near the threshold, improved numerical procedures for the calculation of the single derivative coupling matrix elements are highly desirable.

ACKNOWLEDGMENTS

Support by the Volkswagenstiftung is gratefully acknowledged. Thanks are due to S. Peyerimhoff for providing the quantum chemical programs and to B. Hess for his help in the practical application.

[1] D. L. Lambert, Phys. Scr. **T47**, 186 (1993).
[2] H. Holweger, Phys. Scr. **T65**, 151 (1996).
[3] I. Fleck, J. Grosser, A. Schnecke, W. Steen, and H. Voigt, J. Phys. B **24**, 4017 (1991).
[4] M. F. Mott and H. S. W. Massey, *The Theory of Atomic Collisions* (Clarendon, Oxford, 1949).
[5] J. Grosser, Z. Phys. D **3**, 39 (1986).
[6] J. B. Delos, Rev. Mod. Phys. **53**, 287 (1981).
[7] O. Mo, A. Riera, and M. Yanez, Phys. Rev. A **31**, 3977 (1985).
[8] M. Gargaud, R. McCarroll, and P. Valiron, J. Phys. B **20**, 1555 (1987).
[9] H. Croft and A. S. Dickinson, J. Phys. B **29**, 57 (1996).
[10] J. Grosser, T. Menzel, and A. K. Belyaev, Phys. Rev. A **59**, 1309 (1999).
[11] M. S. Child, *Molecular Collision Theory* (Academic, London, 1974).
[12] J. Grosser, A. Schnecke, and H. Voigt, Z. Phys. D **17**, 251 (1990).
[13] J. Grosser and H. Sturk, Z. Phys. D **35**, 81 (1995).
[14] A. K. Belyaev and J. Grosser, J. Phys. B **29**, 5843 (1996).
[15] R. J. Buenker, S. D. Peyerimhoff, and W. Butscher, Mol. Phys. **35**, 771 (1978).
[16] P. J. Bruna and S. D. Peyerimhoff, Adv. Chem. Phys. **67**, 1 (1987).
[17] D. R. Bates and D. A. Williams, Proc. Phys. Soc. London **83**, 425 (1964).
[18] Yu. N. Demkov, G. V. Dubrovsky, and A. M. Ermolaev, *Abstracts of Papers of the 5th ICPEAC (Leningrad)* (Nauka, Leningrad, 1967), p. 186.
[19] Yu. N. Demkov, C. V. Kunasz, and V. N. Ostrovskii, Phys. Rev. A **18**, 2097 (1978).
[20] M. Ya. Ovchinnikova, Zh. Eksp. Teor. Fiz. **64**, 129 (1973) [Sov. Phys. JETP **37**, 68 (1973)].
[21] R. E. Olson and B. Liu, J. Chem. Phys. **73**, 2817 (1980).
[22] W. C. Stwalley, W. T. Zemke, and S. C. Yang, J. Phys. Chem. Ref. Data **20**, 153 (1991).
[23] R. E. Olson and M. Kimura, Phys. Rev. A **32**, 3092 (1985).
[24] O. Mo and A. Riera, J. Phys. B **25**, L101 (1992).